Ion and Electron Heating Characteristics of Magnetic Reconnection in a Two Flux Loop Merging Experiment

Y. Ono,[1,*] H. Tanabe,[1] Y. Hayashi,[1] T. Ii,[1] Y. Narushima,[2] T. Yamada,[1] M. Inomoto,[1] and C. Z. Cheng[3]
[1]*Graduate School of Frontier Sciences, University of Tokyo, Tokyo, Japan*
[2]*National Institute for Fusion Science, Gifu, Japan*
[3]*Plasma and Space Science Center, National Cheng Kung University, Tainan, Taiwan*
(Received 21 May 2011; published 26 October 2011)

Characteristics of the high-power reconnection heating were measured for the first time directly by two-dimensional measurements of ion and electron temperatures. While electrons are heated mainly inside the current sheet by the Ohmic heating power, ions are heated mainly by fast shock or viscosity damping of the reconnection outflow in the two downstream areas. The magnetic reconnection converts the energy of reconnecting magnetic field B_p mostly to the ion thermal energy, indicating that the reconnection heating energy is proportional to B_p^2.

DOI: 10.1103/PhysRevLett.107.185001 PACS numbers: 52.35.Vd, 52.55.Fa, 52.72.+v

Recent solar observations have shown many signatures of magnetic reconnection heating. The coronal loop-top hard x-ray spot is considered to be a fast shock formed in the downstream of reconnection outflow [1], and the V-shape region of high electron temperature around the X line was interpreted as evidence of slow shock structure around the X line [2]. However, those interpretations are still under serious debate, and more direct evidence is needed to explain the causes and mechanisms for flare heating. Since 1986, the TS-3 toroidal plasma merging experiments have been conducted to study plasma heating effects of magnetic reconnection [3–10]. As shown in Fig. 1, two toroidal plasmas (flux tubes) with major radius $R \sim 0.2$ m were merged together in the axial (Z) direction under magnetic compression provided by the two poloidal field (PF) or acceleration coils. The magnetic reconnection occurs at the contacting point of the two toroidal plasmas, causing high-power plasma heating by magnetic reconnection. The magnetic configurations of the merging toroidal plasmas are the same as general merging flux tubes with varying guide field and have been used widely for formation of ultrahigh-beta field-reversed configuration [6–9] and high-beta spherical tokamak (ST) plasmas [9–12] and for leading the ST experiments to the largest merging experiment Mega Amp Spherical Tokamak [12–14].

An important question then arises as to how and why the reconnection process converts the reconnecting magnetic field energy into ions and electron thermal energies. It is noted that the particle heating mechanism, which is essential for understanding the high-power reconnection heating, is left unsolved. This Letter addresses (i) where ions and electrons are heated by magnetic reconnection, (ii) why ions are heated in the downstream, (iii) why electrons are heated inside the current sheet, and (iv) how the reconnection heating scales with controllable parameters. We found for the first time that strong ion heating is caused by the reconnection outflow in the downstream of the magnetic reconnection region and electron heating occurs inside the reconnecting current sheet.

The TS-3 device has demonstrated the merging or reconnection heating of helium plasmas for high-beta tokamak (toroidal plasma with guide field) formation [1–8]. Its toroidal vacuum vessel with length of 1 m and diameter of 0.8 m has two PF or acceleration coils for poloidal flux injection. A center coil current I_{tfc} is used to apply an external toroidal (guide) field to the merging toroids. Two toroidal plasmas with $R \approx 0.2$ m and $R/a \approx 1.5$ were merged together in the axial direction [9,10]. Before the

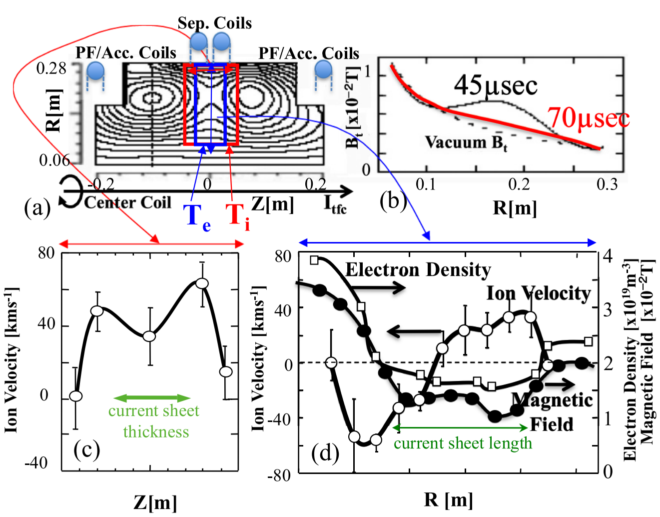

FIG. 1 (color online). (a) Contours of poloidal flux in the poloidal (R-Z) plane and (b) radial toroidal field B_t profiles of two merging high guide-field toroidal plasmas ($I_{tfc} = 35$ kA), which are measured by a 2D magnetic probe array at $t = 45$ μs (and $t = 70$ μs), (c) axial profile of radial reconnection outflow velocity, and (d) radial profiles of radial reconnection outflow velocity, electron density, and magnetic field magnitude at $t = 45$ μs. The outflow profiles are measured by a 1D scan of the Ion Dynamics Spectroscopy Probe.

merging, the two toroidal plasmas were fully ionized and had parameters $T_i \approx T_e \approx 10$ eV, $n_e \approx 2$–5×10^{19} m^{-3}, and $B_t \approx 1.5$ kG. Their merging or reconnection was accelerated by the PF or acceleration coil currents provided by the power crowbar circuit and decelerated by the separation coil currents on the midplane, as shown in Fig. 1(a). The 9×12 arrays of magnetic pickup coils were inserted in the R-Z plane of the vessel to measure directly the 2D magnetic field profile. Its maximum spatial resolution is 30 mm in the radial direction and 5 mm in the axial direction, and its time resolution is 0.5 μs. The poloidal flux contours, current density profiles, and plasma pressure profiles, based on the force balance assumption, were calculated from the measured 2D magnetic field profiles. The current sheet was identified by the measured toroidal current density profile j_t and the X-line structure.

A new 2D ion temperature T_i diagnostics was developed by combining the Doppler broadening measurement with the tomography technique [15,16]. The 2D (7×5) line-integrated data of HeII spectral lines were measured by 35 optical fibers, polychromators, and ICCD cameras. At first, they were transformed into local line spectra in the R-Z plane because the Abel inversion converted the line-integrated emission into local emission at each wavelength. Then, each Doppler width of the spectral line was calculated by using the Gaussian function fitting algorithm to plot the 2D profile of T_i in the R-Z plane. Its spatial resolution is 35 mm in the radial direction and 20 mm in the axial direction, and its time resolution is 2 μs. The 2D electron temperature profile was also measured by a scan of a 1D (5 channels) electrostatic probe array inserted in the R-Z plane. Its radial and axial resolutions are 35 and 10 mm, respectively, and its time resolution is 0.5 μs. Triple probes were used to measure the electron temperature T_e and density n_e without assuming the plasma reproducibility.

Figure 1(a) shows the poloidal flux contours in the poloidal (R-Z) plane of two merging toroidal plasmas whose center q value was about 2. These two toroidal plasmas were merged together due to their parallel plasma currents and reversed currents of PF or acceleration coils. Their reconnection time was as short as 20 μs, which almost equals to the Sweet-Parker reconnection time with the measured effective resistivity. As shown in Fig. 1(b), the large paramagnetic toroidal magnetic field of initial toroidal plasmas was suppressed to the vacuum toroidal field level by the large pulsed plasma heating of reconnection or merging. About 20% of the magnetic energy of the merging toroidal plasmas was converted mainly into ion thermal energy. Figures 1(c) and 1(d) show the axial (Z) and radial (R) profiles of ion velocities measured by the Ion Dynamics Spectroscopy Probe [17] during the toroidal plasma merging. They clearly show the bipolar reconnection outflow from the current sheet in the R direction, in agreement with the conventional reconnection model.

A new finding is that the magnetic reconnection process heats ions in the downstream area and electrons in the current sheet, respectively. The top panels of Fig. 2 show the time evolution of the 2D ion temperature T_i contour during and after the plasma merging. The corresponding 2D poloidal flux contours measured by the 2D magnetic probe array are shown in the bottom panels of Fig. 2. During the reconnection, two hot spots were clearly formed in the two downstream areas of reconnection. The ion temperature in the current sheet was higher than that of the upstream area but was still lower than that in the downstream area. The high ion temperature area expands along the magnetic field lines, forming a four-leg high temperature area. The most probable interpretation for this phenomenon is that the bipolar reconnection outflows collide with the plasma in the closed (reconnected) field lines surrounding the hot spots. This suggests that some damping mechanism of the reconnection outflow must exist in the downstream area.

The hard x-ray image of solar flares also revealed similar hot spots in the downstream area [1]. Although the solar observations cannot measure directly ion temperature profile around the reconnection region, our experimental results suggest that a similar damping mechanism of reconnection outflow can cause the coronal heating. As shown in Fig. 2, the heated ions spread out along the flux surfaces and were mostly confined inside the produced toroidal plasma after merging. In Fig. 1(b), the large paramagnetic B_t of merging toroidal plasmas observed at 45 μs was fully suppressed in the produced toroidal plasma at 70 μs, in agreement with the measured increase in β from 5% to 40%. It is noted that the two hot T_i areas in the downstream are fully surrounded by the thick closed flux surfaces. It is simply because the reconnection proceeds from the peripheral field lines to the core field lines

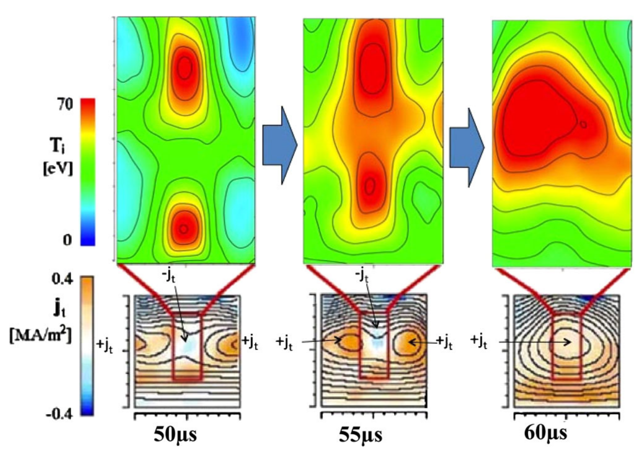

FIG. 2 (color online). R-Z contours of ion temperature during high-guide field toroidal plasma merging ($I_{\rm tfc} = 35$ kA), which was reconstructed from 2D Doppler broadening measurement (top) and corresponding 2D contours of poloidal fluxes measured by a 2D magnetic probe array in the R-Z plane (bottom).

in the case of two flux-loop merging. The ions heated by reconnection are confined after the completion of merging, in sharp contrast with the anomalous ion heating observed in reversed field pinch plasmas. The sawtooth activities in reversed field pinch plasmas tend to reconnect the internal field lines to the open field lines outside the separatrix, losing most of ions heated by the reconnection.

As shown in Figs. 1(c) and 1(d), the maximum outflow speed is about 40 km/s, which is about 70%–80% of the local Alfvén speed. In Fig. 1(d), the bipolar outflow is accelerated up to 40 km/s on both sides of the current sheet and then decreases sharply to values smaller than 3 km/s forming a shock structure at around $R = 0.13$ and 0.24 m. Around these points, the electron density n_e and magnetic field amplitude change in phase with the magnetic field strength as shown in Fig. 1(d). Note that the ratio of electron density jump n_{e1}/n_{e2} is equal within 20% to that of magnetic field jump B_1/B_2, in agreement with the Rankine-Hugoniot relation for the fast shock. The radial profile of ion temperature has double peaks around these fast shock points in the downstream, suggesting the shock or viscosity heating of reconnection outflow. The fast shock and/or the ion viscosity are the most probable cause of the damping of reconnection outflow. The measured heating power ~4 MW roughly agrees with that of reconnection outflow.

Another finding is that electrons are heated inside the current sheet unlike ions. Figure 3 shows contours of electron temperature T_e in the R-Z plane during the high guide-field toroidal plasma merging. A scan of the electrostatic probe array was used to measure the blue-line squared area in Fig. 1(a). While T_e outside the current sheet is uniform at 5–6 eV, it clearly peaks inside the current sheet. We measured the effective resistivity (toroidal electric field divided by toroidal current density at the X point) of the current sheet of high guide-field toroidal plasmas, which is about the same as or 1.5 times larger than the classical resistivity. The Ohmic heating is the most probable cause for the electron heating inside the current sheet. Figure 4 shows the time evolution of the averaged T_i and T_e and total thermal energy calculated from these temperature profiles. It is noted that electrons are heated earlier than ions. While electrons are quickly heated by Ohmic heating in the current sheet, the conversion of the reconnection outflow energy into the ion thermal energy needs more time. The viscosity or shock heating by the reconnection outflow is the most probable cause for the anomalous ion heating. The ion heating power ~4 MW was an order of magnitude larger than the electron heating power ~0.2 MW.

The next question is how the heating energy of the reconnection or merging process scales for various plasma conditions. Figure 5 shows the increment of ion temperature ΔT_i during the magnetic reconnection as a function of the reconnecting field $B_\parallel$. The experimentally measured core ion temperatures are also plotted in the no-guide-field case (counterhelicity merging) and in the high-guide-field case (toroidal plasma merging). It clearly shows that the ion temperature increment ΔT_i as well as ion thermal energy increment ΔW_i increase with $B_\parallel^2$, under a constant density condition. The magnetic reconnection converts the

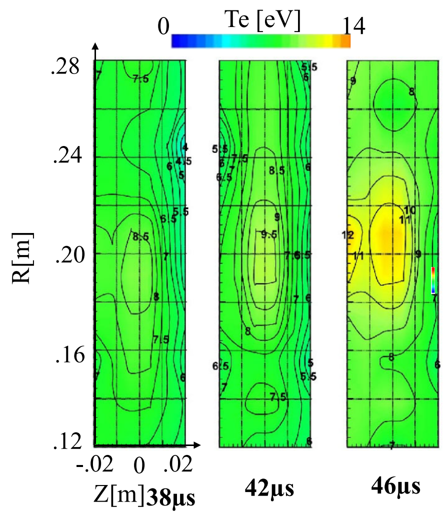

FIG. 3 (color online). R-Z contours of electron temperature around the current sheet during high guide-field toroidal plasma merging ($I_{\rm tfc} = 35$ kA).

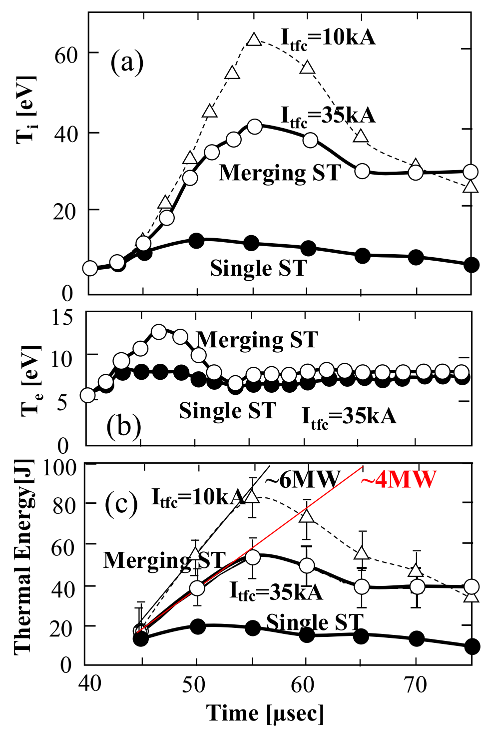

FIG. 4 (color online). Time evolutions of averaged ion and electron temperatures T_i and T_e, respectively, and total thermal energies of single and merging high-guide-field toroidal plasma with $I_{\rm tfc} = 35$ kA. Those for low-guide-field toroidal plasma with $I_{\rm tfc} = 10$ kA are shown by dotted lines.

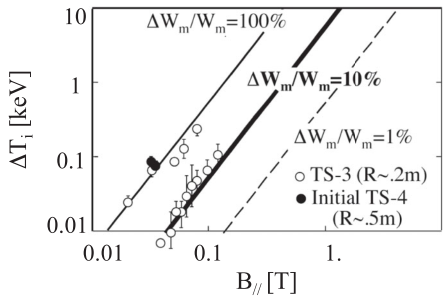

FIG. 5. Ion temperature increments ΔT_i of two merging toroidal plasmas with constant density $n_i \approx 3 \times 10^{19}\ \mathrm{m}^{-3}$ as a function of reconnecting magnetic field $B_{\|}$. The data points were obtained from two merging toroids with and without guide field in TS-3 and initial TS-4 experiments.

reconnecting magnetic field energy of merging toroids into the ion thermal energy. However, it depends on the guide toroidal field B_t. The reconnection outflow speed theoretically equals to the Alfvén speed V_A, when the guide (toroidal) field B_t is zero. The counterhelicity merging of two spheromak plasmas (toroidal plasma with low guide field) with an opposing toroidal field has zero B_t at the X line, and its outflow was as fast as the Alfvén speed, in agreement with the theoretical prediction [18]. The ion viscosity and/or fast shock are considered to convert the outflow kinetic energy into the ion thermal energy $\Delta W_{\mathrm{th}} \approx \Delta W_i$. This result indicates that the ion temperature increment T_i and the thermal energy increment ΔW_{th} scale with $B_{\|}^2$ or V_A^2, as shown in the following equations:

$$\Delta T_i \approx \alpha\beta m_i V_A^2/k = \alpha\beta B_{\|}^2/\mu_0 n_i k$$

and

$$\Delta W_{\mathrm{th}} \approx \Delta W_i = 3/2 \int n_i k \Delta T_i dx^3 = \alpha \Delta W_m = \alpha\beta W_m$$
$$= \alpha\beta \int B_{\|}^2/2\mu_0 dx^3,$$

where n_i, $B_{\|}$, α, and β are the ion density, reconnecting component of magnetic field, conversion efficiency of the dissipated magnetic energy ΔW_m into the ion thermal energy ΔW_i ($0 \leq \alpha \leq 1$), and ratio of ΔW_m to the reconnecting field energy W_m ($0 \leq \beta \leq 1$), respectively. The plasma size is fixed in this $B_{\|}$ scan experiment, indicating that the total energy of reconnecting magnetic field scales with $B_{\|}^2$. Since both ΔT_i and the outflow speed decrease with the guide field B_t, the β parameter represents the outflow slowdown effect of B_t. The α parameter also includes the thermal energy degradation (typically $\alpha = 0.7$–0.9 for tokamak plasmas: toroidal plasma with high guide field) during the merging process. In TS-3, $\alpha\beta$ was measured to increase from 0.1 to 0.8 with decreasing q_0 from 3 to 0.5.

In summary, we have studied the characteristics, causes, and mechanisms for ion and electron heatings during magnetic reconnection in the merging tokamak (toroidal plasma with guide field) experiment by measuring the 2D ion and electron temperature profiles. The 2D ion temperature (T_i) profile was measured by a new type of 2D Doppler tomography diagnostics composed of polychromators with ICCD cameras, optical fibers, and a lens system. The 2D electron temperature profile was measured by the scan of 1D electrostatic probes. The magnetic reconnection process heats plasma ions around the two downstream areas by converting the reconnection outflow energy into the ion thermal energy. The fast shock structure was observed around the hot T_i areas, indicating the most probable dumping mechanism for reconnection outflow. On the other hand, electrons are heated in the current sheet, indicating that the Ohmic heating in the sheet current is the most probable cause for the electron heating. The ion heating power is an order of magnitude higher than the electron heating power, while the electron heating occurs earlier than the ion heating, probably because the ions are heated by the outflow damping process, which occurs later. These heating characteristics are observed widely in the merging toroidal plasmas with varied guide field. The plasma heating results should be generally applicable to the general reconnection magnetic field configurations. The heating power was observed to increase with the external compression force for the merging toroidal plasmas and inversely with the toroidal (guide) magnetic field. It is noted that the reconnection converts a part of the poloidal magnetic energy into ion and electron energies within the short Sweet-Parker reconnection time. This energy conversion transforms the low-β toroidal (tokamak) plasmas ($\beta \sim 5\%$) into a high-β one ($\beta \sim 40\%$).

This work is supported by a Grant-in-Aid for Scientific Research (A) No. 22246119 and (B) No. 19340170, JSPS Core-to-Core Program No. 22001, and NIFS Collaboration Research Programs (NIFS06KOAH02 and NIFS08KUTR023). We acknowledge collaboration and useful discussion with Dr. M. Yamada and Dr. H. Ji of Princeton Plasma Physics Laboratory.

*ono@k.u-tokyo.ac.jp

[1] S. Masuda *et al.*, Nature (London) **371**, 495 (1994).
[2] T. Shimizu *et al.*, Astrophys. J. **422**, 906 (1994).
[3] Y. Ono, A. Yumoto, and M. Katsurai, in *Proceedings of the 1986 IEEE International Conference on Plasma Science, Saskatoon, Canada, 1986* (IEEE, New York, 1986), p. 77.
[4] Y. Ono *et al.*, Phys. Fluids B **5**, 3691 (1993).
[5] M. Yamada, Y. Ono, A. Hayakawa, M. Katsurai, and F. W. Perkins, Phys. Rev. Lett. **65**, 721 (1990).
[6] Y. Ono, M. Yamada, T. Akao, T. Tajima, and R. Matsumoto, Phys. Rev. Lett. **76**, 3328 (1996).
[7] Y. Ono *et al.*, Phys. Plasmas **4**, 1953 (1997).
[8] E. Kawamori and Y. Ono, Phys. Rev. Lett. **95**, 085003 (2005).
[9] Y. Ono and M. Inomoto, Phys. Plasmas **7**, 1863 (2000).

[10] Y. Ono *et al.*, Nucl. Fusion **43**, 789 (2003).
[11] A. Sykes *et al.*, in *Proceedings of the Twenty-first EPS Conference on Controlled Fusion and Plasma Physics* (European Physical Society, Montpellier, 1994), Part I, p. 22.
[12] M. Gryaznevich *et al.*, Phys. Rev. Lett. **80**, 3972 (1998).
[13] A. Sykes *et al.*, in *Proceedings of the Eighteenth International Fusion Energy Conference* (IAEA, Vienna, 2001), OV4/1.
[14] A. Sykes *et al.*, Phys. Plasmas **8**, 2101 (2001).
[15] A. L. Balandin and Y. Ono, Eur. Phys. J. D **17**, 337 (2001).
[16] H. Tanabe *et al.*, IEEJ Trans. Fund. Mater. **130**, 772 (2010).
[17] G. Fiksel, D. J. D. Hartog, and P. W. Fontana, Rev. Sci. Instrum. **69**, 2024 (1998).
[18] E. N. Parker, J. Geophys. Res. **62**, 509 (1957).